tvst

https://doi.org/10.1167/tvst.8.4.20

Article

Vascular Changes in Intermediate Age-Related Macular Degeneration Quantified Using Optical Coherence Tomography Angiography

Matt Trinh[1,2], Michael Kalloniatis[1,2], and Lisa Nivison-Smith[1,2]

[1] School of Optometry and Vision Science, University of New South Wales, Sydney, Australia
[2] Centre for Eye Health, University of New South Wales, Sydney, Australia

Correspondence: Lisa Nivison-Smith, School of Optometry and Vision Science, UNSW Australia, Sydney, 2052, NSW, Australia. e-mail: l.nivison-smith@unsw.edu.au

Received: 21 February 2019
Accepted: 10 June 2019
Published: 7 August 2019

Keywords: optical coherence tomography angiography; age-related macular degeneration; vascular density; retinal vasculature

Citation: Trinh M, Kalloniatis M, Nivison-Smith L. Vascular changes in intermediate age-related macular degeneration quantified using optical coherence tomography angiography. Trans Vis Sci Tech. 2019;8(4):20, https://doi.org/10.1167/tvst.8.4.20

Purpose: To examine changes in retinal vasculature and ganglion cell layer (GCL) thickness in intermediate age-related macular degeneration (AMD) using optical coherence tomography angiography (OCTA).

Methods: Zeiss Cirrus Angioplex OCTA 6 × 6 mm scans and a macula 512 × 128 cube scans of the central retina were taken of 63 eyes with intermediate AMD and 51 control eyes. For OCTA scans, the superficial and deep capillary plexus were automatically segmented and vascular density quantified as total number of pixels contributing to the blood flow signal detectable by OCTA. Images were then skeletonized and vessel length, diameter index, morphology, and branching complexity determined. Foveal avascular zone (FAZ) characteristics and GCL thickness were extracted from in-built Angioplex software.

Results: Vascular density was significantly reduced in the superficial capillary plexus of AMD eyes compared with normal eyes, particularly in the superior quadrant (42.4% ± 1.6% vs. 43.2% ± 1.4%; $P < 0.05$). A nonsignificant reduction was also seen in the deep capillary plexus ($P = 0.06$). Total vessel length and average vessel diameter were all significantly decreased in AMD eyes suggesting density changes were related to decreased vessel number and caliber. Vascular complexity and number of branch points was significantly decreased in the deep capillary plexus ($P < 0.05$) suggesting loss or significantly reduced flow of vessels. Average GCL thickness was also significantly reduced in the AMD eyes ($P < 0.05$). No significant changes in FAZ parameters were observed in AMD eyes.

Conclusions: This study suggests intermediate AMD affects both the quantity and morphology of inner retinal vasculature and may be associated with changes in inner retinal structure. This work builds upon the notion that AMD pathogenesis may extends beyond the outer retina.

Translational Relevance: Better understanding of retinal vascular changes in AMD can provide insights in the development of treatment and prevention protocols for these diseases.

Introduction

Age-related macular degeneration (AMD) is the leading cause of central vision impairment in developed countries.[1] Several studies have implicated the role of vascular changes of the outer retina in the development and progression of AMD. In the choroid, thickness is reduced in both nonneovascular and neovascular AMD[2–5] and angiography shows prolonged choroidal filling phase in early AMD.[6] Choriocapillaris loss is associated also with AMD lesions, drusen, reticular pseudodrusen, and retinal pigment epithelium (RPE) atrophy.[2,4,7] More recent work using optical coherence tomography angiography (OCTA) has found decreased choroidal vessel density in the early stages of AMD[8–11] and subclinical choroidal neovascularization (CNV) lesions in intermediate AMD, not detectable with fluorescein angiography.[12]

Vascular changes within the inner retina also appear to be evident in AMD with reports of increased pulsatility and decreased blood flow velocity in retinal arteries of AMD eyes[5] and both dilation and attenuation of retinal arteriolar and venular width in early AMD.[13–15] Recent work with OCTA has also attempted to describe abnormal retinal vasculature in AMD but exact findings have been inconsistent. Toto et al.[16] reported loss of vascular density in the superficial capillary plexus (SCP) in intermediate AMD, but others have suggested changes are localized only to the deep capillary plexus (DCP) or both layers.[11,17] These discrepancies may be due to limiting OCTA assessment to vascular density (the percentage area within an image attributing to blood vessels) as theoretically, eyes with different vascular arrangements or morphology could yield the same overall vascular density.

Thus, this study undertook an in-depth investigation of the SCP and DCP of eyes with intermediate AMD using OCTA, assessing for vascular density, length, morphology, and overall network attributes such as complexity and branching pattern. Using this approach, we could assess for specific processes such as vessel thinning, selective loss of blood vessels and/or reduced flow, and ensure subtle changes, which may not affect vascular density, can still be detected. Considering structural changes in inner retina have been observed in the early stages of AMD,[8,18–24] we also assess ganglion cell layer (GCL) thickness in our AMD cohort to determine if there is an association between changes in vasculature supplying this region that may contribute to our understanding of the pathogenesis of AMD.

Materials and Methods

Study Population

All patient data were obtained through retrospective analysis of records from July 1, 2016, to February 28, 2018, of patients attending the Centre for Eye Health (CFEH) Sydney, Australia, for a macula assessment. CFEH is a referral-only clinic providing advanced diagnostic eye testing by specially trained optometrists and ophthalmologists.[25] Details of macula assessment provided by CFEH have been previously described and include a standard history questionnaire, visual function assessment (visual acuity, contrast sensitivity, Amsler grid), dilated funduscopy, retinal photography, optical coherence tomography (OCT), OCTA, and fundus autofluorescence.[26] All patients had given prior written consent to use their data for research in accordance with the Declaration of Helsinki and approved by the Biomedical Human Research Ethics Advisory Panel of the University of New South Wales.

A patient's record was considered for the control group if the record indicated eyes showed no evidence of ocular disease including subretinal or intraretinal deposits, lesions, fluid, pigment, or vascular changes at the macula. A patient's record was considered for the AMD group if one of the eyes had been diagnosed with intermediate AMD based on evaluation of fundus photography, scanning laser ophthalmoscopy photography, and OCT using the Ferris classification system.[27] Grading of AMD within the record was performed by the examining clinician and reviewed by a second, nonblinded clinician. If there was a disagreement, a third clinician (ophthalmologist) was consulted. Consistent with our previous studies,[28–30] a subset of cases used in the study were re-reviewed independently by an ophthalmologist to confirm accuracy of the original diagnosis listed in the record. Any records where patients had a refractive error greater than ± 5 diopters were excluded to minimize image magnification error, which may impact OCTA measurements.[31,32] Complete characteristics of both cohorts are given in Table 1.

OCTA Image Acquisition

For all included records, OCTA images were acquired using the Zeiss Cirrus Angioplex OCTA (Carl Zeiss Meditec, Jena, Germany). This commercially available, spectral-domain OCT performs 68,000 A-scans per second and is based on a proprietary "OMAG" algorithm. Scans are accompanied by "Fasttrac," a fixation-tracking software, and also a motion correction algorithm. Scans with significant artefacts (such as large floaters, segmentation errors, and blinking or motion artefact) or signal strength of lower than 8 were excluded.[33]

Images were acquired as 6 × 6 mm volume scans centered on the fovea. For this scan area, each B-scan contains 350 A-scans spaced 17.1 μm apart in the horizontal and vertical direction. Following extraction of images from records, vascular layers were automatically segmented based on the Zeiss Cirrus Angioplex algorithm with the SCP (between the inner limiting membrane [ILM] to the inner plexiform layer [IPL]) and DCP (between the inner nuclear layer [INL] to the outer plexiform layer [OPL]) extracted for analysis (Fig. 1). Note, the inbuilt Cirrus projection removal tool was applied to all DCP

Table 1. Subject Demographics

	Normal	Intermediate AMD	*P* Value
Eyes, *n*	51	63	
Age (y)			
Mean	64.70	67.80	0.07[a]
Range	52 to 80	50 to 80	
Sex (%)			
Males	26	35	0.17[a]
Females	25	28	
Eye (%)			
Right	22	32	0.56[a]
Left	29	31	
BCVA			
Mean	6/6	6/6	0.32[b]
Range	6/15 to 6/3	6/12 to 6/4	
Rx (D)			
Mean	−0.36	0.31	0.19[b]
Range	−3.75 to +2.50	−3.25 to +4.00	

BCVA, best corrected visual acuity; Rx (D), refractive error (diopters).

[a] Fisher exact test.

[b] Mann-Whitney *t*-test.

images before analysis. Image quality and segmentation was assessed by two independent graders (MT, LNS) and any eyes showing significant inaccuracies were excluded from further analysis.

OCTA Image Analysis

For the foveal avascular zone (FAZ), values for the total area, perimeter, and circularity were extracted for the central avascular area in OCTA images of the SCP using in-built software of Zeiss Cirrus Angioplex (Figs. 2C, 2D). FAZ axis ratio was determined as the ratio of the major axis length to minor axis length of an ellipse fit to the FAZ region based on previous studies[34] using external software, ImageJ (National Institutes of Health, Bethesda, MD). The latter measurement was included due to its consistency regardless of axial length and refractive error between eyes.

For retinal vasculature, OCTA en face images of the SCP and DCP (Fig. 1) were exported and converted to 8-bit binary using ImageJ. Images were then locally thresholded using a mean formula, and a threshold radius of 400 μm to minimize the appearance of artefacts. Vascular parameters were then determined as described in Chu et al.[35] Briefly, vascular density was quantified as the percentage of

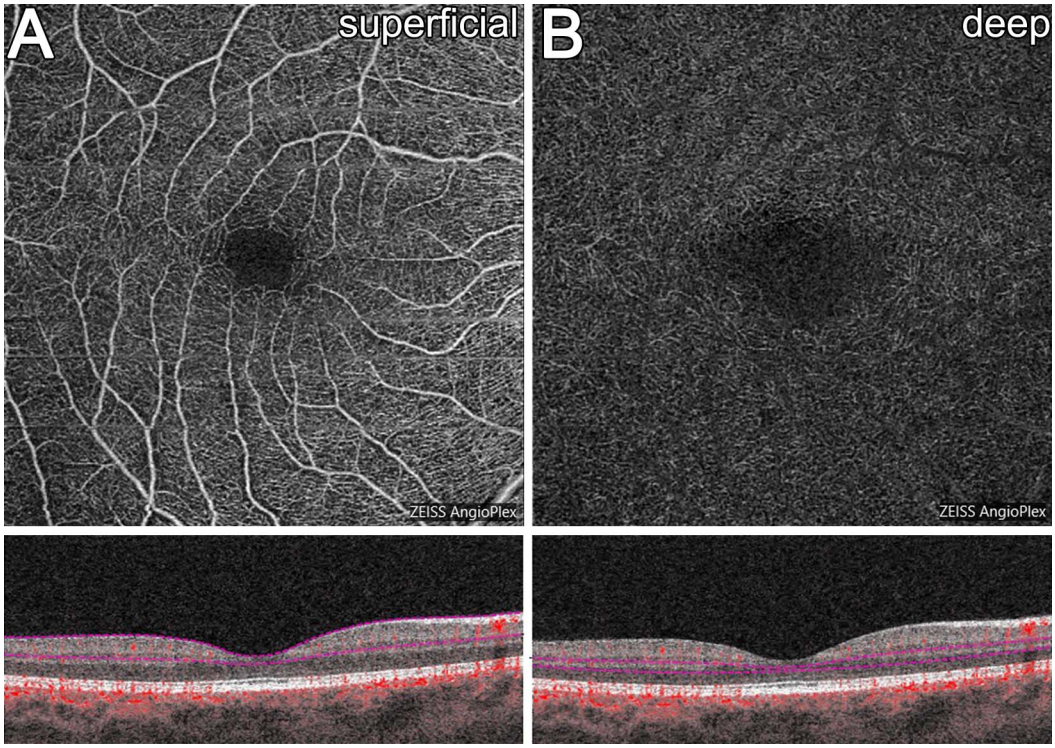

Figure 1. En face and B-scan representations of the (A) SCP and (B) DCP quantified in this study.

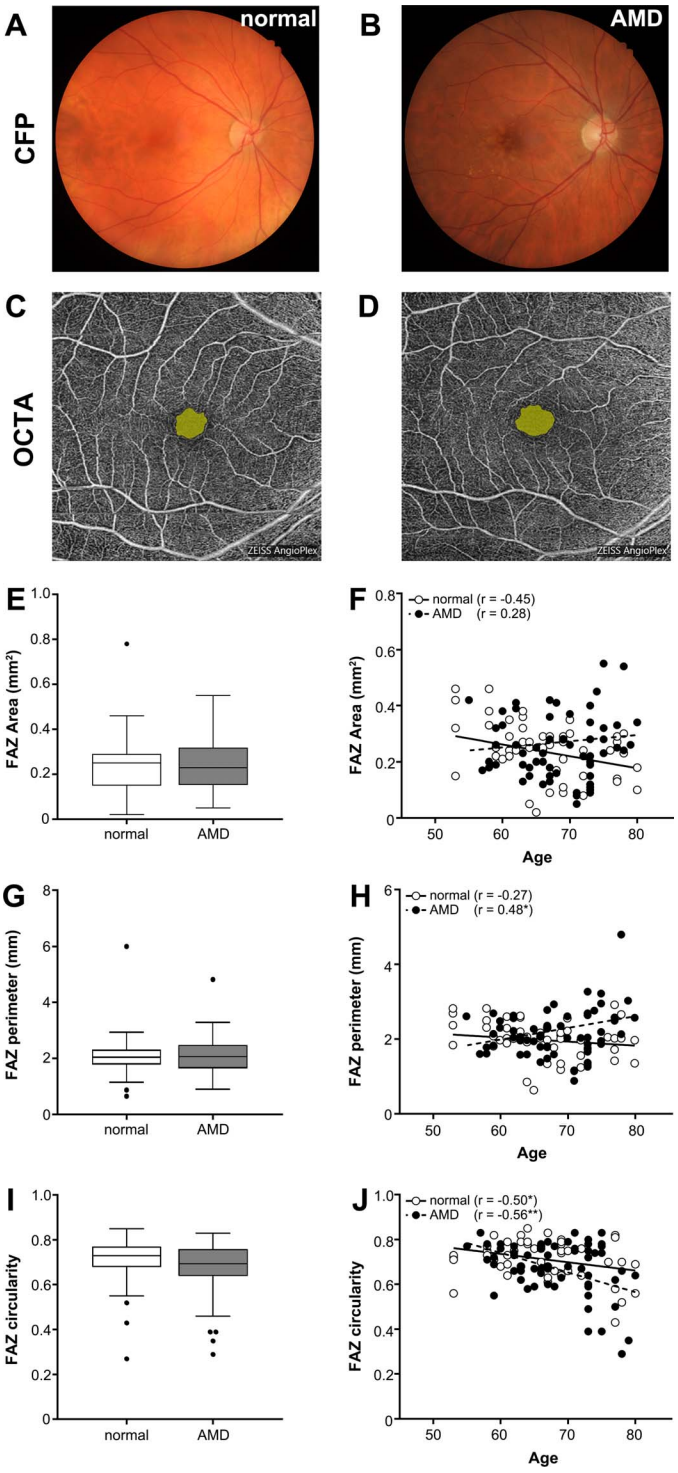

Figure 2. Examples of normal and AMD eyes using (A, B) color fundus photography (CFP) and (C, D) en face OCTA of the SCP with FAZ highlighted in yellow. FAZ (E) area, (F) perimeter, (G) circularity, and (I) axis ratio were assessed for all normal and AMD eyes. *Box* and *whisker plots* represent Tukey method (where the *whiskers* extend to 1.5 × IQR, and values exceeding this are plotted as individual points).

pixels attributing to blood flow signal over total area in the thresholded OCTA image (examples in Figs. 3A, 3B). Vessel length was determined by subjecting images to skeletonized transformation where all vessels were converted to a single pixel width (examples in Figs. 3E, 3F) then quantifying the number of pixels attributing to blood vessels. Vessel diameter index (VDI) was determined by dividing vascular density by vessel length to indicate average diameter of vessels in the OCTA image. Finally, vascular complexity index (VCI) was determined based on dividing the square of the total vessel perimeter over 4*π*vascular density to indicate the relative complexity of the vascular network.

Branching analysis was performed on skeletonized OCTA images using the "Analyze Skeleton" tool in ImageJ. This analysis classified each voxel contributing to blood vessels as either branches, junctions, or endpoints based on having two neighboring voxels, more than 2 neighboring voxels, or less than 2 neighboring voxels, respectively (see example in Fig. 6A).

GCL Thickness Analysis

Macular 512 × 128 cube scans (128 B-scans, each comprising 512 A-scans) obtained on the Cirrus HD-OCT (Carl Zeiss Meditec) at the same time as the OCTA images were extracted. Scans were inspected for quality and segmentation, and GCL thickness was extracted from the GCL analysis module available through the in-built software.

Statistical Analysis

Statistical analysis of categorical subject demographics was performed using a Fisher exact test and continuous measurements with a Mann-Whitney *t*-test. Analysis of OCTA parameters and GCL thickness between eyes was performed using 2-way analysis of variance (ANOVA) with the Sidak multiple comparisons test for posthoc analysis or *t*-test where appropriate. All analysis was conducted using GraphPad Prism (v7, GraphPad Software, Inc., La Jolla, CA) and significance was considered as $P < 0.05$.

Results

Subject Demographics

Fifty-one eyes from 33 healthy individuals and 63 eyes from 41 intermediate AMD subjects were

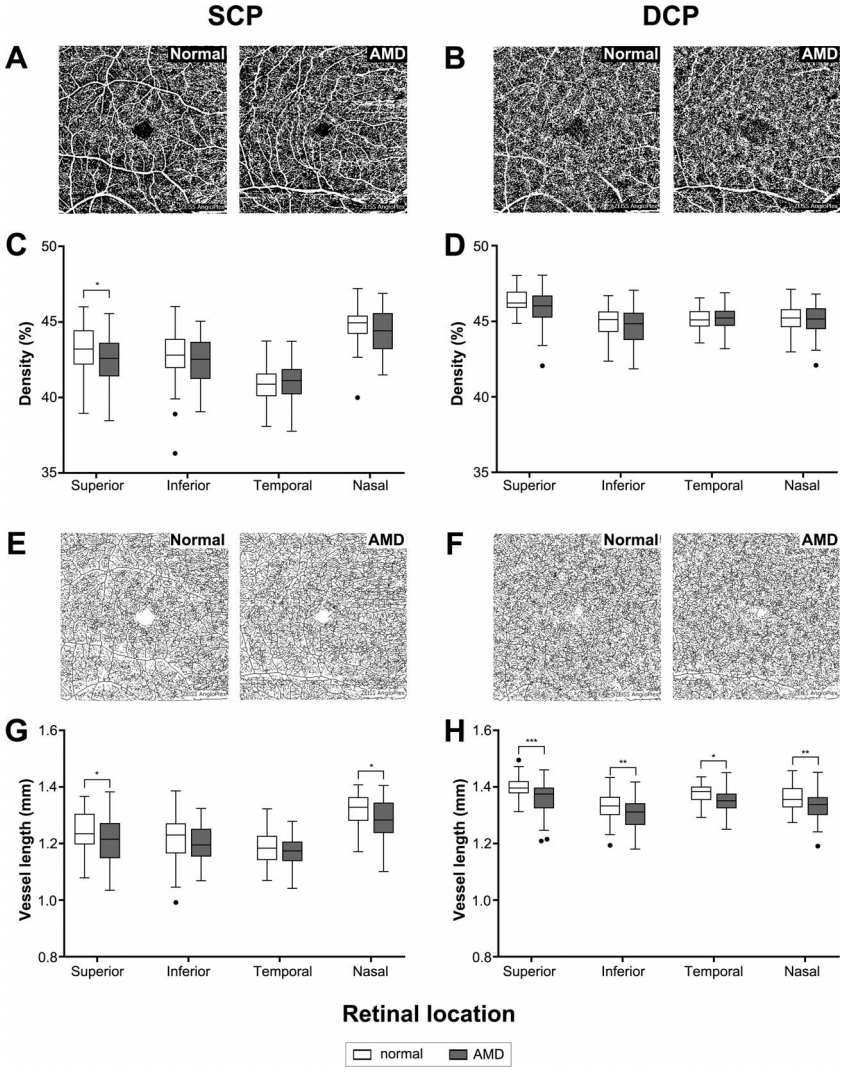

Figure 3. (A, B) Examples of thresholded OCTA images used to quantify vascular density and (C, D) resulting measurements for each quadrant for the (C) SCP and (D) DCP. Thresholded images then underwent (E, F) skeletonized transformation to determine total vessel length in the (G) SCP and (H) DCP. *Box* and *whisker plots* represent Tukey method (where the *whiskers* extend to 1.5 × IQR, and values exceeding this are plotted as individual points). *$P < 0.05$; **$P < 0.01$; ***$P < 0.001$.

assessed in the study. There was no significant difference between eyes of subjects, and data were matched for age and sex between normal and intermediate AMD cohorts (Table 1).

FAZ Characteristics

There was no significant difference between normal and AMD eyes in terms of FAZ total area, perimeter, or circularity when quantified from the en face SCP slab by in-built manufacturer software (*t*-test, $P = 0.12$–0.89; Figs. 2E–2G). FAZ axis ratio, a FAZ measurement that is not affected by ocular magnification,[36] also showed no significant difference between the two cohorts (*t*-test, $P = 0.89$; Fig. 2H).

Vascular Density, Length, and Diameter

Vascular density was determined from the total area within the OCTA image contributing to blood flow signal (Figs. 3A, 3B). Density was significantly reduced between AMD eyes and normal eyes in the SCP (2-way ANOVA, $P < 0.05$) with posthoc analysis indicating significance in the superior quadrant (Sidak multiple comparisons test, superior: $P < 0.05$; Fig. 3C). A reduction was seen in the DCP, but this did not reach significance (2-way ANOVA, $P = 0.06$; Fig. 3D).

Total vessel length (based on skeletonized images; Figs. 3E, 3F) was also significantly decreased in AMD eyes compared with normal eyes in both retinal layers

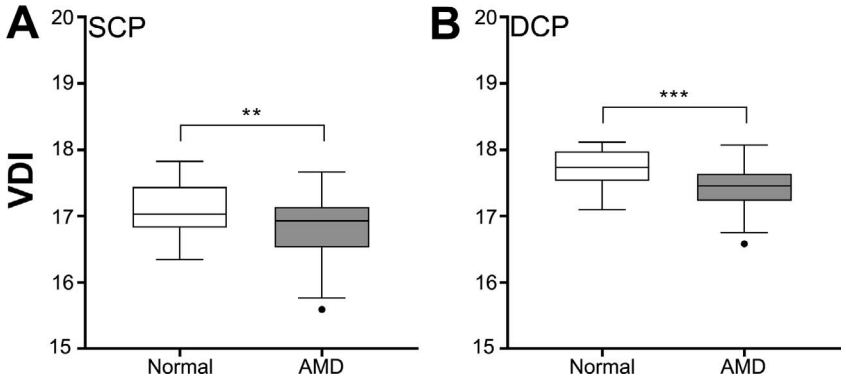

Figure 4. Vascular diameter index (VDI) for normal and AMD eyes in the (A) SCP and (B) DCP. *Box* and *whisker plots* represent Tukey method. $^{**}P < 0.01$; $^{***}P < 0.001$.

(2-way ANOVA, $P < 0.001$ for SCP and DCP). Posthoc analysis revealed significant change across most quadrants (Sidak multiple comparisons test, $SCP_{superior}$: $P < 0.01$; SCP_{nasal}: $P < 0.05$; $DCP_{superior}$: $P < 0.001$; $DCP_{inferior}$: $P < 0.01$; $DCP_{temporal}$: $P < 0.05$; DCP_{nasal}: $P < 0.01$; Figs. 3G, 3H). Vascular density and length measurements of the SCP produced by the inbuilt software of the Cirrus OCTA device demonstrated complementary findings (Supplementary Fig. S1). Together, these results suggested the decrease in vascular density in AMD was due, in part, to loss of retinal vessels.

Aside from vessel length, changes in vascular density can also occur due to changes in vessel caliber. Thus, we assess the average vessel diameter through VDI. VDI was significantly decreased in AMD eyes compared with normal eyes in both the SCP and DCP (Student's *t*-test, SCP: $P < 0.01$, DCP: $P < 0.001$; Fig. 4) suggesting decrease in vascular density in AMD eyes was also in part due to thinning or constriction of existing blood vessels.

Vascular Morphology

To further investigate the origins of vascular changes in AMD, the morphology and overall complexity of the retinal vasculature were quantified. The complexity of the vasculature (as quantified by the VCI described by Chu et al.[35]) was reduced in AMD eyes compared with normal eyes in both capillary layers (Student's *t*-test, SCP: $P < 0.05$, DCP: $P < 0.001$; Fig. 5). This was supported by branching analysis of the skeletonized images of OCTA images, which found a significantly reduced number of branches, junctions, and endpoints in AMD eyes compared with normal eyes and in the DCP (Figs. 6A–6D). The average branch length of AMD eyes was also significantly greater than normal eyes indicating fewer branch points (Student's *t*-test, $P < 0.001$; Figs. 6E, 6F).

GCL Thickness Analysis

Finally, to see if retinal vascular changes may be associated with other structural abnormalities in

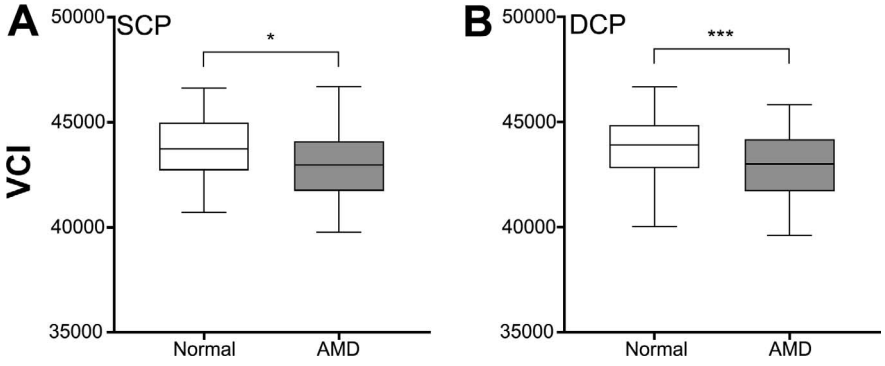

Figure 5. Vascular complexity index (VCI) for normal and AMD eyes in the (A) SCP and (B) DCP. *Box* and *whisker plots* represent Tukey method. $^{*}P < 0.05$; $^{***}P < 0.001$.

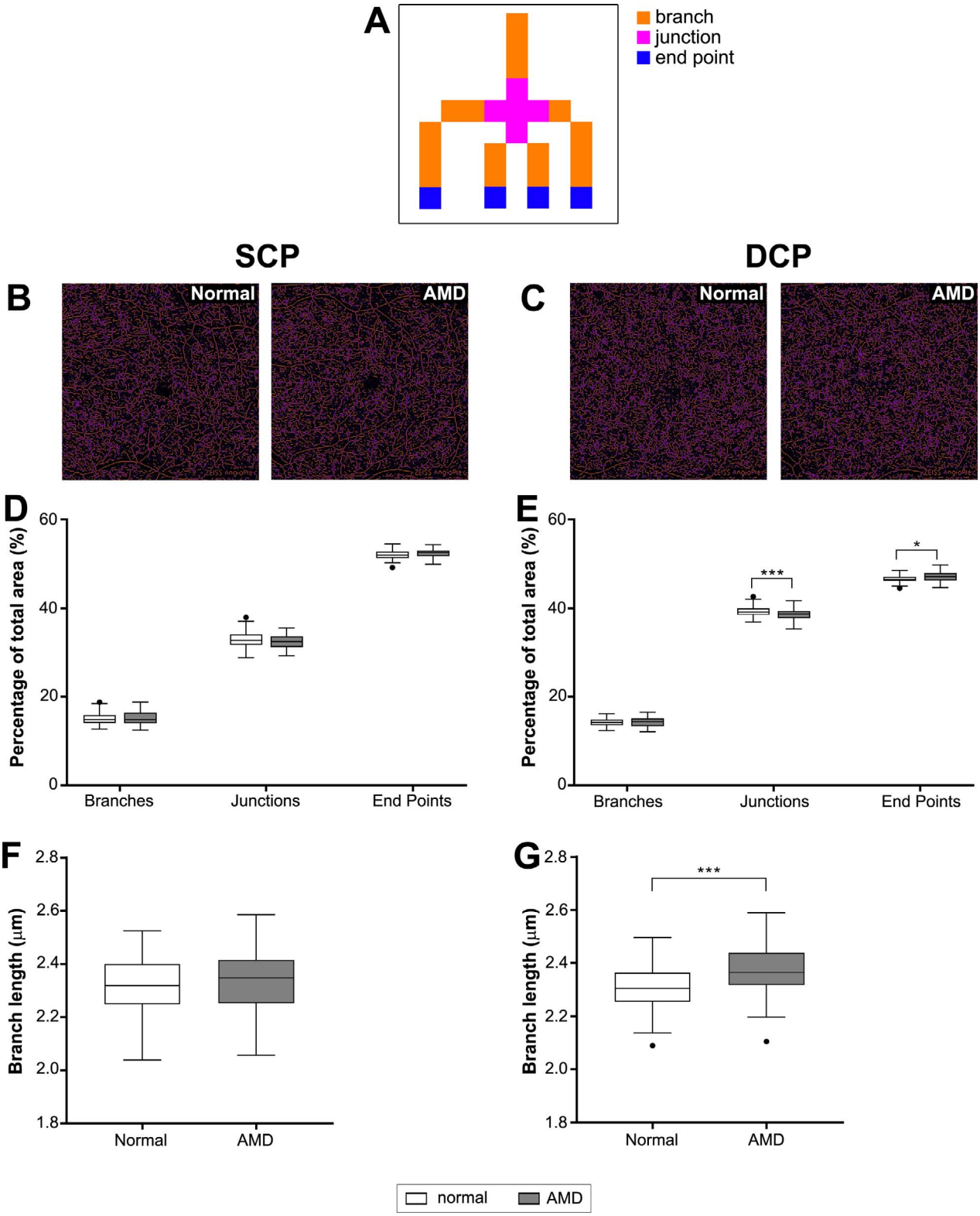

Figure 6. Vessel branching analysis. (A) Diagram of classification for branching analysis and examples of branching analysis for skeletonized images of the (B) SCP and (C) DCP. Note voxels were defined as branches (*orange*) if they had exactly two neighbors, junctions (*purple*) if they had three or more neighbors, and endpoints (*blue*) if they had less than two neighbors. (D, E) The mean number of each voxel type and (F, G) the average branch length was then plotted for the (D, F) SCP and (E, G) DCP. $^{**}P < 0.01$; $^{***}P < 0.001$.

Table 2. GCL Thickness Analysis

	Normal	Intermediate AMD	*P* Value
Average GCL thickness	79.1 ± 8.2	77.5 ± 8.4	0.18[a]
Minimum GCL thickness	73.8 ± 14.3	73.5 ± 10.4	0.67[a]
GCL sector (%)			
Superior	79.8 ± 9.6	77.3 ± 9.1	**0.02**[b]
Superotemporal	79.1 ± 10.7	79.2 ± 8.6	
Inferotemporal	77.7 ± 7.4	76.9 ± 8.8	
Inferior	76.0 ± 9.6	75.4 ± 8.4	
Inferonasal	82.5 ± 10.0	78.6 ± 8.9	
Superonasal	82.6 ± 10.3	77.7 ± 8.5	

[a] Student's *t*-test.
[b] Two-way ANOVA.
Bold indicates significant *P* value.

AMD, macular GCL thickness was assessed. Average and minimum GCL thickness showed no significant change between normal and AMD eyes (Table 2). Sectorial analysis, however, revealed a significant decrease in GCL thickness between normal and AMD eyes (2-way ANOVA, $P < 0.01$; Table 2).

Discussion

This study describes the vascular changes in eyes with intermediate AMD using OCTA. Our study found vascular density was significantly decreased in the SCP but not the DCP. Vessel length, diameter, and complexity were also reduced suggesting loss of vascular density was potentially due to both a change in quantity and morphology of the inner retinal vasculature in AMD eyes. This is consistent with previous literature, which has demonstrated vascular changes in the early stages of AMD are not limited to the choroidal blood supply.[16,17,37] We also observed a loss in GCL thickness in AMD eyes suggesting retinal vascular changes may be associated with structural loss in the early stages of AMD.

Vascular Density Was Reduced in Intermediate AMD

This study found significant loss of vascular density of the SCP in AMD eyes compared with control eyes and a trend for the DCP. This reflects some of the previous literature, specifically Toto et al.[16] who reported reduced vascular density in intermediate AMD in the superficial plexus only. Cicinelli et al.[17] on the other hand reported a significant reduction in vascular density in the deep plexus only. The discrepancy between OCTA studies may be device related as various OCTA modalities use different scanning protocols and different definitions to automatically segment retinal vasculature. Indeed, Magrath et al.[38] assessed a cohort of normal individuals and found significant differences in FAZ area and vascular density measurements with different OCTA devices. Lee et al.[11] found significant change in both vascular layers in early AMD eyes where the fellow eye had progressed to neovascular AMD, suggesting that as the disease progresses the entire retinal vasculature is altered. This is supported by associations of vascular density with markers of AMD progression such as reticular pseudodrusen, outer retinal atrophy, and nascent geographic atrophy.[11,17,39,40] Decreased retinal vasculature may be a response to a reduced metabolic demand from the inner retina due to thinning of the IPL and GCLs in AMD.[18–24] Alternatively, degeneration of inner retina vasculature may cause ischemia in these areas, leading to inner retinal thinning.[8] Assessment of inner retinal thinning was beyond the scope of this study but could be implemented easily in the future considering the integration of OCT and OCTA in a single device.

AMD Affects Both Quantity and Morphology of Inner Retinal Vasculature

Vessel length, diameter, and complexity were all reduced in AMD eyes compared with normal eyes. This suggested that, at least in part, loss of vascular density was due to changes in the number of vessels in the scan area as well as their caliber. Inherent limitations with OCTA means that it is difficult to determine whether absence of vessels is due to actual loss or decreased blood flow, which makes the vessels beyond the threshold of detection for OCTA. Remsch et al.,[41] however, found no change in blood flow volume or velocity in retinal capillaries in early AMD eyes, supporting the former.

Similarly, our diameter measurements only indicate an average across the scan area and therefore it is difficult to confirm if reduced VDI was due to constriction of existing vessels or a shift in average vessel diameter as a consequence of reduced vessel length. This measurement also does not truly describe how different vasculature subsets such as veins, venules, arteries, arterioles, and capillaries may have altered individually. In diabetic retinopathy, decreases in vascular density and vessel length observed on

OCTA are usually accompanied with an increase in average VDI reflecting the loss in smaller caliber vessels.[42] Our vascular complexity and branching analysis also suggests inner retinal change in AMD may be localized to the microvasculature, but we observed a decrease in VDI suggesting average diameter changes were not likely a consequence of vessel loss but rather a shift in average vessel profile. Assessment of retinal photos also support the notion of arterial narrowing in early AMD although this finding has been inconsistent.[14,15]

FAZ Was Not Altered in Intermediate AMD

Several studies indicate retinal pathology including AMD is associated with altered FAZ area or perimeter.[17,43–46] However, in this study, we observed no difference in average FAZ parameters in AMD eyes compared with normal eyes. Few other studies have focused on FAZ parameters beyond area in AMD, although loss of FAZ circularity has been associated with presence of central visual field defects in glaucoma and GCL thickness in diabetic retinopathy,[47,48] supporting the notion that beyond area, irregularity in the geometry of the FAZ may be worth consideration in disease management. Parameters such as circularity and axis ratio are also less affected by factors such as axial length, making them useful in clinical practice.

Vascular Changes May Be Associated With Structural Changes in The Inner Retina in AMD

A number of structural changes have been observed in the inner retina in the early stages of AMD including loss of GCL, IPL, and ganglion cell complex (GCC) thickness.[8,18–24] We found a significant decrease in GCL thickness between normal and AMD eyes in our study, suggesting changes in the vasculature supplying the inner retina could be associated with structural consequences. Reasons for this are unknown, but reduced retinal blood supply to inner retinal neurons in AMD eyes could lead to ischemia and cell loss. Alternatively, others have shown correlations between outer and inner retinal changes in AMD,[8,20] speculating photoreceptor loss leads to redundancy in inner retinal neuron circuitry and subsequent cell loss. In this case, alterations in retinal vasculature could be a response to reduced inner retinal demand. Determining the exact relationship between structural and vascular components of the inner retina in AMD was beyond the scope of the current study, but future studies could correlate these factors with known outer retinal lesions of AMD to provide better insight into the mechanism of vascular alteration in early AMD.

Limitations

There were several limitations in this study. Firstly, as OCTA is a relatively recent development, standards relating to image acquisition and segmentation are still being developed, making it difficult to establish procedures for developing normative data for vascular density. For example, while most OCTAs claim to separate the superficial and deep plexus, anatomically, there is also an intervening intermediate plexus, which is not resolved by conventional OCTA algorithms. Campbell et al.[49] demonstrated that current arbitrary segmentation of the superficial and deep vascular plexus at the inner nuclear/plexiform border leads to inconsistent contributions of the intermediate capillary plexus to these layers. New nomenclature proposing the superficial and deep vascular complexes (to account for the intermediate capillary plexus) may clarify these issues and ensure OCTA findings are consistent with histological findings in the future.

Further to this, automated segmentation of retinal layers by OCTA devices has been flagged as a significant area of concern, particularly considering reports of layer segmentation commonly requiring manual correction in AMD eyes.[30,50] In this study, we reviewed segmentation of the SCP and DCP, amending layer segmentation as necessary but were limited in the extent of manual correction due to limitations in the Zeiss OCTA Angioplex. This, however, may not have been a significant issue as Brandl et al.[50] indicated that despite differences in layer thickness in AMD eyes using automated and manual segmentation, the overall significant changes associated with disease were still detectable with either measure. Furthermore, the group noted the RPE and Bruch's membrane layer segmentation were the only layers to show significant effects of segmentation errors whilst this work assessed the SCP and DCP, which concerned segmentation of the inner retina (specifically the ILM, INL, and OPL).

In this study, we chose to use a 6×6 mm scan protocol available on the Zeiss Cirrus Angioplex. This protocol has a lower resolution than other scan protocols available on this instrument and may not have revealed all vasculature within the central retina. However, the larger area visible in this scanning protocol makes it useful in a clinical setting and

therefore demonstrating this protocol can still detect significant differences in retinal vasculature in AMD may have greater translational value.

Only a single OCTA device was used for assessment. Although several studies have compared different OCTA devices,[38,51] most do so with normal populations and therefore their findings may not translate to diseased eyes. Comparative analysis suggests the Zeiss device used in this study ranks superior to other OCTA devices in terms of fewer image artefacts and better vessel continuity.[51] Specifically, the "OMAG" algorithm employed by the Zeiss device improves visualization of retinal microvascular image contrast and vessel connectivity and therefore may have allowed better detection of subtle vascular changes in AMD. The Zeiss device, however, is associated with spectral-domain OCTs and is limited in terms of reduced penetration, increased signal attenuation, and sensitivity roll-off toward deeper retinal lesions. Thus, future studies using newer swept-source OCTs and artefact-reducing algorithms may provide further insight into vascular changes in AMD.

Additionally, we did not correct for magnification errors from varying axial lengths, which have been shown to affect FAZ measurements.[31,32] We did, however, exclude subjects' spherical equivalent refraction over 5 diopters as refractive error is considered to have the strongest correlation with axial length than any other ocular components such as cornea and crystalline lens, and should place magnification errors within less than 15% for all subjects.[32]

Conclusion

This study used OCTA to characterize vascular changes in eyes with intermediate AMD. We found vascular density was significantly reduced in the SCP in intermediate AMD compared with age- and sex-matched normal eyes. This change appeared to be related to loss in vessel quantity and morphology. We also found loss in GCL thickness, suggesting vascular changes in the inner retina in AMD could have structural associations. These results build upon previous work, suggesting a role for the inner retinal blood supply in the pathogenesis of AMD.

Acknowledgments

The authors thank Judy Nam for technical assistance.

This work was supported in part by Guide Dogs NSW/ACT through support for LN-S and the Centre for Eye Health, a joint initiative with UNSW Sydney.

Authors LNS and MK are named inventors on a patent relating to eye imaging (Australian Provisional Patent Application No. 2018901002).

Disclosure: **M. Trinh**, None; **M. Kalloniatis**, Bio-Imaging of the Eye Using Pattern Recognition (No. 2018901002; P); **L. Nivison-Smith**, Bio-Imaging of the Eye Using Pattern Recognition (No. 2018901002; P)

References

1. Wong WL, Su X, Li X, et al. Global prevalence of age-related macular degeneration and disease burden projection for 2020 and 2040: a systematic review and meta-analysis. *Lancet Glob Health*. 2014;2:e106–e116.
2. Mullins RF, Johnson MN, Faidley EA, et al. Choriocapillaris vascular dropout related to density of drusen in human eyes with early age-related macular degeneration. *Invest Ophthalmol Vis Sci*. 2011;52:1606–1612.
3. Lee JY, Lee DH, Lee JY, et al. Correlation between subfoveal choroidal thickness and the severity or progression of nonexudative age-related macular degeneration. *Invest Ophthalmol Vis Sci*. 2013;54:7812–7818.
4. McLeod DS, Grebe R, Bhutto I, et al. Relationship between RPE and choriocapillaris in age-related macular degeneration. *Invest Ophthalmol Vis Sci*. 2009;50:4982–4991.
5. Friedman E, Krupsky S, Lane AM, et al. Ocular blood flow velocity in age-related macular degeneration. *Ophthalmology*. 1995;102:640–646.
6. Pauleikhoff D, Spital G, Radermacher M, et al. A fluorescein and indocyanine green angiographic study of choriocapillaris in age-related macular disease. *Arch Ophthalmol*. 1999;117:1353–1358.
7. Garg A, Oll M, Yzer S, et al. Reticular pseudodrusen in early age-related macular degeneration are associated with choroidal thinning. *Invest Ophthalmol Vis Sci*. 2013;54:7075–7081.
8. Borrelli E, Abdelfattah NS, Uji A, et al. Postreceptor neuronal loss in intermediate age-related macular degeneration. *Am J Ophthalmol*. 2017;181:1–11.

9. Cicinelli MV, Rabiolo A, Marchese A, et al. Choroid morphometric analysis in non-neovascular age-related macular degeneration by means of optical coherence tomography angiography. *Br J Ophthalmol*. 2017;101:1193–1200.
10. Chatziralli I, Theodossiadis G, Panagiotidis D, et al. Choriocapillaris vascular density changes in patients with drusen: cross-sectional study based on optical coherence tomography angiography findings. *Ophthalmol Ther*. 2018;7:101–107.
11. Lee B, Ahn J, Yun C, et al. Variation of retinal and choroidal vasculatures in patients with age-related macular degeneration. *Invest Ophthalmol Vis Sci*. 2018;59:5246–5255.
12. Roisman L, Zhang Q, Wang RK, et al. Optical coherence tomography angiography of asymptomatic neovascularization in intermediate age-related macular degeneration. *Ophthalmology*. 2016;123:1309–1319.
13. Yang K, Zhan SY, Liang YB, et al. Association of dilated retinal arteriolar caliber with early age-related macular degeneration: the Handan Eye Study. *Graefes Arch Clin Exp Ophthalmol*. 2012; 250:741–749.
14. Wang JJ, Mitchell P, Rochtchina E, et al. Retinal vessel wall signs and the 5 year incidence of age related maculopathy: the Blue Mountains Eye Study. *Br J Ophthalmol*. 2004;88:104–109.
15. Liew G, Kaushik S, Rochtchina E, et al. Retinal vessel signs and 10-year incident age-related maculopathy: the Blue Mountains Eye Study. *Ophthalmology*. 2006;113:1481–1487.
16. Toto L, Borrelli E, Di Antonio L, et al. Retinal vascular plexuses' changes in dry age-related macular degeneration, evaluated by means of optical coherence tomography angiography. *Retina*. 2016;36:1566–1572.
17. Cicinelli MV, Rabiolo A, Sacconi R, et al. Retinal vascular alterations in reticular pseudodrusen with and without outer retinal atrophy assessed by optical coherence tomography angiography. *Br J Ophthalmol*. 2018;102:1192–1198.
18. Camacho P, Dutra-Medeiros M, Paris L. Ganglion cell complex in early and intermediate age-related macular degeneration: evidence by SD-OCT manual segmentation. *Ophthalmologica*. 2017;238:31–43.
19. Muftuoglu IK, Ramkumar HL, Bartsch DU, et al. Quantitative analysis of the inner retinal layer thicknesses in age-related macular degeneration using corrected optical coherence tomography segmentation. *Retina*. 2018;38:1478–1484.
20. Lee EK, Yu HG. Ganglion cell-inner plexiform layer and peripapillary retinal nerve fiber layer thicknesses in age-related macular degeneration. *Invest Ophthalmol Vis Sci*. 2015;56:3976–3983.
21. Savastano MC, Minnella AM, Tamburrino A, et al. Differential vulnerability of retinal layers to early age-related macular degeneration: evidence by SD-OCT segmentation analysis. *Invest Ophthalmol Vis Sci*. 2014;55:560–566.
22. Yenice E, Sengun A, Soyugelen Demirok G, et al. Ganglion cell complex thickness in nonexudative age-related macular degeneration. *Eye (Lond)*. 2015;29:1076–1080.
23. Zucchiatti I, Parodi MB, Pierro L, et al. Macular ganglion cell complex and retinal nerve fiber layer comparison in different stages of age-related macular degeneration. *Am J Ophthalmol*. 2015; 160:602–607.
24. Lamin A, Oakley JD, Dubis AM, et al. Changes in volume of various retinal layers over time in early and intermediate age-related macular degeneration. *Eye (Lond)*. 2019;33:428–434.
25. Jamous KF, Kalloniatis M, Hennessy MP, et al. Clinical model assisting with the collaborative care of glaucoma patients and suspects. *Clin Exp Ophthalmol*. 2015;43:308–319.
26. Ly A, Nivison-Smith L, Hennessy MP, et al. Collaborative care of non-urgent macular disease: a study of inter-optometric referrals. *Ophthalmic Physiol Opt*. 2016;36:632–642.
27. Ferris FL 3rd, Wilkinson CP, Bird A, et al. Clinical classification of age-related macular degeneration. *Ophthalmology*. 2013;120:844–851.
28. Nivison-Smith L, Milston R, Chiang J, et al. Peripheral retinal findings in populations with macular disease are similar to healthy eyes. *Ophthalmic Physiol Opt*. 2018;38:584–595.
29. Nivison-Smith L, Wang H, Assaad N, et al. Retinal thickness changes throughout the natural history of drusen in age-related macular degeneration. *Optom Vis Sci*. 2018;95:648–655.
30. Rogala J, Zangerl B, Assaad N, et al. In vivo quantification of retinal changes associated with drusen in age-related macular degeneration. *Invest Ophthalmol Vis Sci*. 2015;56:1689–1700.
31. Linderman R, Salmon AE, Strampe M, et al. Assessing the accuracy of foveal avascular zone measurements using optical coherence tomography angiography: segmentation and scaling. *Transl Vis Sci Technol*. 2017;6:16.
32. Sampson DM, Gong P, An D, et al. Axial length variation impacts on superficial retinal vessel density and foveal avascular zone area measurements using optical coherence tomography angiography. *Invest Ophthalmol Vis Sci*. 2017;58: 3065–3072.

33. Al-Sheikh M, Ghasemi Falavarjani K, Akil H, et al. Impact of image quality on OCT angiography based quantitative measurements. *Int J Retina Vitreous*. 2017;3:13.
34. Linderman RE, Muthiah MN, Omoba SB, et al. Variability of foveal avascular zone metrics derived from optical coherence tomography angiography images. *Transl Vis Sci Technol*. 2018;7:20.
35. Chu Z, Lin J, Gao C, et al. Quantitative assessment of the retinal microvasculature using optical coherence tomography angiography. *J Biomed Opt*. 2016;21:66008.
36. Krawitz BD, Mo S, Geyman LS, et al. Acircularity index and axis ratio of the foveal avascular zone in diabetic eyes and healthy controls measured by optical coherence tomography angiography. *Vision Res*. 2017;139:177–186.
37. Lee B, Ahn J, Yun C, et al. Variation of retinal and choroidal vasculatures in patients with age-related macular degeneration. *Invest Ophthalmol Vis Sci*. 2018;59:5246–5255.
38. Magrath GN, Say EAT, Sioufi K, et al. Variability in foveal avascular zone and capillary density using optical coherence tomography angiography machines in healthy eyes. *Retina*. 2017;37:2102–2111.
39. Toto L, Borrelli E, Mastropasqua R, et al. Association between outer retinal alterations and microvascular changes in intermediate stage age-related macular degeneration: an optical coherence tomography angiography study. *Br J Ophthalmol*. 2017;101:774–779.
40. Ahn SM, Lee SY, Hwang SY, et al. Retinal vascular flow and choroidal thickness in eyes with early age-related macular degeneration with reticular pseudodrusen. *BMC Ophthalmol*. 2018; 18:184.
41. Remsch H, Spraul CW, Lang GK, et al. Changes of retinal capillary blood flow in age-related maculopathy. *Graefes Arch Clin Exp Ophthalmol*. 2000;238:960–964.
42. Kim AY, Chu Z, Shahidzadeh A, et al. Quantifying microvascular density and morphology in diabetic retinopathy using spectral-domain optical coherence tomography angiography. *Invest Ophthalmol Vis Sci*. 2016;57:OCT362–OCT370.
43. Takase N, Nozaki M, Kato A, et al. Enlargement of foveal avascular zone in diabetic eyes evaluated by en face optical coherence tomography angiography. *Retina*. 2015;35:2377–2383.
44. Di G, Weihong Y, Xiao Z, et al. A morphological study of the foveal avascular zone in patients with diabetes mellitus using optical coherence tomography angiography. *Graefes Arch Clin Exp Ophthalmol*. 2016;254:873–879.
45. Freiberg FJ, Pfau M, Wons J, et al. Optical coherence tomography angiography of the foveal avascular zone in diabetic retinopathy. *Graefes Arch Clin Exp Ophthalmol*. 2016;254:1051–1058.
46. Kwon J, Choi J, Shin JW, et al. Glaucoma diagnostic capabilities of foveal avascular zone parameters using optical coherence tomography angiography according to visual field defect location. *J Glaucoma*. 2017;26:1120–1129.
47. Kim K, Kim ES, Yu SY. Optical coherence tomography angiography analysis of foveal microvascular changes and inner retinal layer thinning in patients with diabetes. *Br J Ophthalmol*. 2018;102:1226–1231.
48. Kwon J, Choi J, Shin JW, et al. Alterations of the foveal avascular zone measured by optical coherence tomography angiography in glaucoma patients with central visual field defects. *Invest Ophthalmol Vis Sci*. 2017;58:1637–1645.
49. Campbell JP, Zhang M, Hwang TS, et al. Detailed vascular anatomy of the human retina by projection-resolved optical coherence tomography angiography. *Sci Rep*. 2017;7:42201.
50. Brandl C, Brücklmayer C, Günther F, et al. Retinal layer thicknesses in early age-related macular degeneration: results from the German AugUR Study Retinal Layer Thicknesses in Early AMD. *Invest Ophthalmol Vis Sci*. 2019;60:1581–1594.
51. Munk MR, Giannakaki-Zimmermann H, Berger L, et al. OCT-angiography: a qualitative and quantitative comparison of 4 OCT-A devices. *PLoS One*. 2017;12:e0177059.